



COBEM
2021 Florianópolis - Brasil



26th ABCM International Congress of Mechanical Engineering
November 22-26, 2021. Florianópolis, SC, Brazil

COBEM2021-1513

SIGNAL TREATMENT AND ANALYSIS OF A LOW COST STRAPDOWN INERTIAL MEASUREMENT UNIT

Aline Peres Leal

Department of Naval and Oceanic Engineering
Polytechnic School of the University of São Paulo
aline.peresleal@usp.br

André Luís Condino Fuarra

Department of Mobility Engineering
Federal University of Santa Catarina
andre.fuarra@ufsc.br

Abstract. *Flow-induced vibration (FIV) of submerged structures (e.g. risers, pipelines, tendons, mooring lines) is a complex fluid-structure interaction, where the relation between forces and responses is extensively investigated. The design of these structures needs to be carefully analyzed to avoid large amplitudes of motion that lead to a short life in fatigue and risk of accidents. Also, field monitoring is necessary to evaluate the real behavior of these bodies submitted to currents, waves, drift movement of the platform, among other excitations. Current equipment for such monitoring are very robust and expensive. This work aims to initiate the investigation of a low-cost sensing unit for this application, using MEMS accelerometers, rate gyros, and magnetometers in a strapdown inertial measurement unit (IMU). The inertial unit is composed using Arduino electronic prototyping platform and an IMU module called GY-87 10DOF. Calibration and sensitivity factors are applied. Then, preliminary signals from this IMU, containing simple rotation movements, are treated and filtered through different techniques in Octave, using rotations matrix, quaternions, and sensorial fusion with complementary and Kalman filter, in order to have cleaner results to analyze. The results obtained applying these different procedures are compared and discussed. Then, the main objective is to choose the best method to handle data from the low-cost sensor and then apply these steps in future FIV experiments data.*

Keywords: *IMU, sensorial fusion, Kalman filter, monitoring, FIV.*

1. INTRODUCTION

Flexible risers have become key components in production through floating structures. With floating production systems being deployed in deeper waters and under more adverse climatic conditions, special attention must be paid to the dynamic behavior, resistance and service life of the risers.

The dynamic behavior of the riser is excited by external forces, as movements of the platform, waves, and currents. The response is determined by material and geometry properties and by the reactive forces of the fluid. The movement response in these cases is not well defined, in this way, a good excitation-response relationship prediction of deep-sea technologies such as risers, underwater pipelines, and sub-sea structures must be established to get a reliable design.

Although the studies made in the design process, e.g. (Morooka and Tsukada, 2013; Ramos and Pesce, 2004; Pesce and Martins, 2005), it is known that the operating behavior may have some particular aspects. The measurement and monitoring of these submerged systems is a significant aspect related to the offshore dynamics and, at the same time, the instruments for this application can be very expensive.

The monitoring of a structure is related to the positions tracking, verifying the occurrence of damages and an eventual need for interventions. This task involves data collection in the field, its processing, and analysis in the laboratory. The monitoring system involves a set of sensors responsible for converting physical parameters into electrical signal. This electrical signal can be connected to an amplifier or converter, and then be sent to a data acquisition system, in which the signal is stored and analyzed. In addition, the quantity to be monitored needs to be evaluated according to the objective.

Related to the sub-sea monitoring sensors, in the paper of Mukundan *et al.* (2010), it was implemented a reconstruction of the riser motion related to vortex-induced vibration (VIV). It was used a limited number of sensors placed along its length, including strain gauges and accelerometers. It was concluded that the results were dependent on the number of sensors used and on reconstruction using a database. Lavieri (2011) in his master dissertation, studied the inertial navigation method applied to sub-sea launches. He analyzed accelerometers and rate gyros, applying scripts to treat the

signal and the errors from the components. With this structure, he has got relatively good predictions, but without sensory fusion, the results still showed drift.

Driessen *et al.* (2018) studied the sensor fusion to determine the velocity and position of an unmanned aerial vehicle (UAV) using low-cost sensors. The sensorial fusion was done with Extended Kalman Filter (EKF), applied to an Inertial Measurement Unit (IMU), an optical-flow sensor, and a sonar. The results were estimated without drift and validated with data provided by a motion-capture system. Applying optical-flow and sonar sensors resulted in better estimation for velocity and position. For military operations in urban areas, Vissière *et al.* (2007) analyzed the problem of position estimation for a rigid body, in an indoor situation, using an inertial measurement unit (IMU) and a set of four spatially distributed magnetometers, applying EKF to do the sensor fusion. They found that the variations of the magnetic field can actually be used to improve the position estimation. Liu *et al.* (2019) utilized the EKF to fuse the multi-source information, including depth information from a pressure sensor, pose from IMU, velocity from optical flow and pose estimation from multiple planar markers, and they have found highly accurate results.

As the first step for predicting positions involves calculating the body's orientation, only this stage is also analyzed in some works. Romaniuk and Gosiewski (2014), applied Kalman filter to treat orientation and position, using GPS to do the position correction. The orientation filtering algorithm showed measurement noise reduction and resolution increase. Liu *et al.* (2014) studied attitude estimation for agricultural robot with mean filter and a Kalman filter, and the estimation precision was improved. Gui *et al.* (2015) investigated real time tilting measurement using an IMU. Complementary and Kalman Filter were applied and were able to obtain smooth and accurate results. Barrera *et al.* (2018) studied the sensor fusion using only Kalman Filter and demonstrated the good reduction of noise in the orientation signals when applying this type of filter.

In this context, the present work aims to investigate sensors in a low-cost IMU. The data processing and analysis of the sensors behavior is an important step before conduct experiments. Then, accelerometers, rate gyros, and magnetometers are evaluated and have their signals treated through different techniques in order to show which is the most suitable treatment for such IMU. The main contribution of this work is to present a clear methodology to begin the work involving a low-cost IMU, comprising the steps of calibration, analysis of the results obtained, and application of filters.

2. INERTIAL SENSORS

Sensors are devices that respond to a stimulus in a specific way, producing a signal that can be converted and interpreted by other devices. Inertial sensors are sensors that calculate the forces acting in a body based on Newton's First Law of Motion. Accelerometers and rate gyros are typical examples of inertial sensors. An IMU is an electronic device that measures and reports a body's specific force and angular rate using a combination of accelerometers and rate gyros. Often, magnetometers are used as auxiliary sensors for the inertial system, especially for heading estimation.

The strapdown technology is present in modern navigation systems such as an IMU. In this technology, sensors are attached rigidly to the body, being lower cost and smaller than the platform systems, enabled by Micro-Electro-Mechanical Systems (MEMS). MEMS are the integration of mechanical elements, actuators, sensors, and electronic components, arranged on a substrate of microscopic proportions, e.g., silicon plate.

The module GY-87, Figure 1, is used in this work. It is an IMU composed by 3 accelerometers and 3 rate gyros in the sensor called MPU-6050, 3 magnetometers in the digital compass called HMC5883 and a digital barometric pressure sensor BMP180 which gives temperature and pressure values. In the next section, specifications of these sensors (rate gyro, accelerometer and magnetometer) will be given. The representation of the rotation angles that are going to be presented, in the three-body axes, can be seen in Figure 2.

There are many other types of inertial sensors and auxiliaries, that can be utilized to estimate position, velocity, orientation, acceleration. In all the cases, the first procedure is always to do the transformation between coordinates systems, using the relative angles between them. Usually, this transformation is from the sensor system to the Earth frame. Therefore, this work will study the sensor orientation, which will have applications in any type of subsequent navigation data.



Figure 1. GY-87 10DOF module. Size compared with a coin.

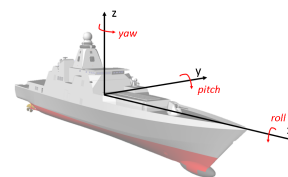


Figure 2. Angle representation.

The rate gyro, a specific type of gyroscope, measures rotational velocity or rate of change of the angular position over

time, along the x , y , and z axis in the 3D system. The rate gyro can be modeled as:

$$\tilde{\omega}_n = \frac{\omega_n + b_n^g + \eta_n^g}{\text{sensitivity factor}} \quad (1)$$

where n is the component analyzed, $\tilde{\omega}$ is the read value, ω is the true angular velocity, b^g is the rate gyro bias, and η^g the additive, zero-mean Gaussian, rate gyro noise. Bias error can be considered as constant and removed using calibration. The additive noise is random and usually corrected through filters. There are other kinds of noises, but these are the most significant. This sensor model, as well as the others presented below, is a simplified model which does not consider cross-axis sensitivity, cross-coupling, and misalignment, etc.

Rate gyros can measure the rotation of Earth, i.e. around $0.004^\circ/s$. If the sensor is not so accurate, which is the case of the MEMS sensors, it does not pick this rotation rate. Usually, noise is bigger than the Earth rotation rate in MEMS sensors.

The outputs of the rate gyro are in degrees per second so, to get the angular position it is necessary to integrate angular velocity, as follows:

$$\phi_k = \phi_{k-1} + \dot{\phi}\Delta t \quad (2)$$

being ϕ the roll angle, $\dot{\phi} = \omega_x$ the angular velocity on the x-axis, k is the iteration. The same is valid for the other angles, as shown in Figures 2, where θ , ψ , are pitch and yaw angles, $\dot{\theta} = \omega_y$, $\dot{\psi} = \omega_z$ the other angular velocities. This process is called dead reckoning. To reduce the error generated by noise during the integration, which is the drift error, it is necessary to use a high baud rate and filter the signal. Table 1 contains the MPU6050 rate gyro characteristics used in this work, according to the datasheet.

2.1 Accelerometer

The accelerometer can measure gravitational acceleration along the axes x , y , z , being a_x , a_y e a_z , respectively. The accelerometer model is:

$$\tilde{a}_n = \frac{a_n^g + a_n^t + b_n^a + \eta_n^a}{\text{sensitivity factor}} \quad (3)$$

where a^g is the gravitational acceleration, a^t external accelerations (related to forces), b_n^a is the accelerometer bias and η^a the accelerometer noise. Measures obtained from the accelerometer are accurate in the long term because there is no drift, but they are noisy and unreliable in short-run due to motion.

Using some trigonometry math, it is possible to calculate the angle at which the sensor is positioned, as shown in the following equations:

$$\theta = \text{atan2}\left(-a_x, \sqrt{a_y^2 + a_z^2}\right) \frac{180}{\pi}; \quad (4)$$

$$\phi = \text{atan2}\left(a_y, \sqrt{a_x^2 + a_z^2}\right) \frac{180}{\pi}; \quad (5)$$

With integration in the acceleration vectors, velocity and after translation position can be found. But, again, results are subject to noise problems. There always is drift with dead reckoning. Accelerometer characteristics used in this work are described in Table 1.

2.2 Magnetometer

The magnetometer measures the total magnetic flux density in a given direction in Gauss, M_x , M_y , and M_z for the three perpendicular axes. The magnetometer model is:

$$\tilde{M}_n = \frac{M_n + M_n^s + M_n^h + \eta_n^m}{\text{sensitivity factor}} \quad (6)$$

where M is the true magnetic flux density, M^s and M^h are the soft and hard errors, respectively, and η^m in the magnetometer white noise. Magnetometers need to be calibrated in the field to evaluate hard and soft iron errors.

With geometry, the yaw angle can be predicted with the magnetometer, considering roll and pitch angles (tilt-compensated compass value), as follows (Groves, 2015):

$$X_h = M_x \cos(\theta) + M_y \sin(\phi) \sin(\theta) + M_z \cos(\phi) \sin(\theta) \quad (7)$$

$$Y_h = -M_y \cos(\phi) + M_z \sin(\phi) \quad (8)$$

$$\psi_m = \text{atan2}(Y_h, X_h) \frac{180}{\pi}; \quad (9)$$

where ψ_m is the magnetic heading. The true heading is measured by $\psi_{nb} = \psi_m + \alpha_m$, where α_m is the magnetic declination, according to the local. The magnetometer characteristics are shown in Table 1.

Table 1. Sensors specifications.

Parameter	Rate gyros value	Accelerometers value	Magnetometers value
Sensitivity	± 250 °/s	$\pm 2g$	± 8 gauss
Sensitivity scale factor	131 LSB/(°/s)	16384 LSB/g	1370 LSB/gauss
ADC Word Length	16 bits	16 bits	8 bits

3. DATA ACQUISITION AND ANALYSIS METHOD

Arduino UNO R3 was used to connect the GY-87 module and capture measurements from the sensors. Using the open-source Arduino Software (IDE), the microcontroller was programmed to read the sensors' raw values and record the data in an SD card, in text format. Then, the tests were carried out wireless, using a 9V battery. The output file was composed by time, accelerometers, rate gyros, and magnetometers readings, in each column of data.

After capturing the measurements it is necessary to conduct the signal treatment, apply the sensors factors, correct bias, and deal with the noises.

3.1 Signal Treatment

Octave software was used to read the text file and calculate the accelerations, attitude, and heading, and apply filters to deal with the noises. Firstly, the calibration process was conducted. For that, the sensor was placed on a leveled surface and left standing for a few seconds (60 s). With that, it was possible to calibrate rate gyros, once the angular velocities were zero, disregarding the rate of rotation of the earth, and calibrate accelerometers, knowing that the only acceleration acting is the gravity acceleration and it points down. To calibrate the magnetometer, the sensor was rotated in 360° around each axis, to capture the magnetic field in the location. Putting the z axis perpendicular to the horizontal plane, x and y axes could be calibrated, then positioning either x or y perpendicular to the horizontal plane, z axis could be calibrated. In this calibration process, N samples of the 3 axes were acquired, from which the mean values were obtained to determine the offsets. For the magnetometer, the hard-iron offset was calculated as:

$$M_n^h = \frac{\max(M) + \min(M)}{2} \quad (10)$$

Having the results from calibration it was possible to apply the bias correction (subtract the offset values) and sensitivity factor, or gain, to the raw value read in the sensors, as exposed in Equations 1, 3 and 6. After that, the values were the expected value plus noise and the units were: acceleration in m/s^2 , rotation rate in $^\circ/s$ and, the magnetic field in Gauss. Thus, noise needs to be treated.

The moving mean, a type of low-pass filter, was used. With this, it was possible to minimize the high-frequency noise coming from the sensors. A moving mean with 10 terms was used for a sampling frequency of 250Hz to preserve signal amplitude.

All these signals were collected in the body frame (b), or sensor frame, once the body is the sensor itself. Consequently, if the objective is to find acceleration, velocity, and position of the body, the next step is to transform that to the Earth frame (e), which has its origin at the Earth's center. For that, it is necessary to apply the following relation:

$$[a^e] = [R][a^b] - [G] \quad (11)$$

where a is the acceleration, $[R]$ is the transformation matrix, and $[G]$ is the gravitational acceleration vector.

To find the transformation matrix, it is necessary to deal with the rotations of the sensor. As related before, the main objective of this work is to present attitude and heading readings in a clear signal. For that, it was applied quaternions, sensor fusion with complementary and Kalman filter with Euler angles, in order to compare each one. Sensor fusion is a process that consists of combining information from different sensors, through a fusion mechanism in order to obtain an output signal with better quality that could be obtained from a single sensor, reducing the uncertainty of the estimated sensors' values. The next subsection will present the different approaches to obtain body orientation.

3.1.1 Gyro rates integration

The simplest way to calculate the IMU orientation is by integration of the gyro rates values. Equation 2 can be applied in this process. The initial values $\phi(0)$, $\theta(0)$ and $\psi(0)$ need to be determined to proceed with the integration. For that the initialization process is necessary. As the accelerometers were calibrated, roll and pitch initial angles can be estimated by the relations between the acceleration components. For the yaw angle, magnetometers can be used. The initialization process is also needed in the other process shown below.

Then, having the attitude and heading computed, the transformation matrix from the body frame to earth frame can be written based on the Euler angles as:

$$[R]_b^e = \begin{bmatrix} \cos(\theta)\cos(\psi) & -\cos(\phi)\sin(\psi) + \sin(\phi)\sin(\theta)\cos(\psi) & \sin(\phi)\sin(\psi) + \cos(\phi)\sin(\theta)\cos(\psi) \\ \cos(\theta)\sin(\psi) & \cos(\phi)\cos(\psi) + \sin(\phi)\sin(\theta)\sin(\psi) & -\sin(\phi)\cos(\psi) + \cos(\phi)\sin(\theta)\sin(\psi) \\ -\sin(\theta) & \sin(\phi)\cos(\theta) & \cos(\phi)\cos(\theta) \end{bmatrix} \quad (12)$$

3.1.2 Orientation using quaternions

Euler angles can cause problems for orientation tracking with more than one axis because rotations are not commutative. Quaternions may solve this kind of problem. A quaternion can be described by the equation:

$$q = q_w + iq_x + jq_y + kq_z \quad (13)$$

with a scalar q_w and a vector part q_x, q_y, q_z .

A rotation quaternion has unitary length and it can be constructed from a rotation of θ radians around an axis \mathbf{v} as:

$$q_r(\theta, \mathbf{v}) = \cos(\theta/2) + iv_x\sin(\theta/2) + jv_y\sin(\theta/2) + kv_z\sin(\theta/2) \quad (14)$$

Otherwise, a vector quaternion usually represents a 3D point or a 3D vector, $\mathbf{u} = (u_x, u_y, u_z)$, with scalar part equal to zero:

$$q_u = 0 + iu_x + ju_y + ku_z \quad (15)$$

With the rotation quaternion and the vector quaternion, it is possible to rotate a vector using the following equation:

$$q'_u = q_r q_u q_r^{-1} \quad (16)$$

where q'_u is the rotated vector, similar to the rotation matrix of q multiplied by \mathbf{u} .

Given the output of 3-axis rate gyros, it can be determined the normalized axis of this rotation as $\omega/|\omega|$ and the angle of rotation (in radians) as $|\omega|\Delta t$. Using Equation 13, it is possible to convert this axis-angle representation to a rotation quaternion as:

$$q(\Delta t) = q_r \left(|\omega|\Delta t, \frac{\omega}{|\omega|} \right) \quad (17)$$

here, $q_{\Delta t}$ represents the instantaneous rotation from the local sensor frame at the current time step to the local sensor frame at the last time step.

Thus, it is needed to combine all instantaneous rotations in a time loop as $q(t + \Delta t) = q(t)q(\Delta t)$. After successive rotations, the vector \mathbf{u} can be represented in the earth frame as:

$$q_u^{(e)} = q(t + \Delta t)q_u^{(b)}q(t + \Delta t)^{-1} = q(t)q(\Delta t)q_u^{(b)}q(\Delta t)^{-1}q(t)^{-1} \quad (18)$$

Then, the transformation of coordinate systems was done by applying rotation quaternions.

3.1.3 Complementary Filter

As related before, the orientation angles can be described by the rate gyros signals integrated in time, and, by the equations with the accelerometer and the magnetometer, Section 2. Integrals turn noise into a drift, so it is fundamental to use a high rate to minimize that. However, it is possible to remove drift from gyroscope via a high-pass filter and remove high-frequency noise from accelerometer and magnetometer via low-pass filter, using a complementary filter. Equations 19, 20 and 21 represent the formula for complementary filter to find the angles of roll, pitch and yaw, respectively:

$$\phi_k = \alpha(\phi_{k-1} + \omega_x\Delta t) + (1 - \alpha)atan2 \left(-a_y, \sqrt{a_x^2 + a_z^2} \right) \quad (19)$$

$$\theta_k = \alpha(\theta_{k-1} + \omega_y\Delta t) + (1 - \alpha)atan2 \left(a_x, \sqrt{a_y^2 + a_z^2} \right) \quad (20)$$

$$\psi_k = \alpha(\psi_{k-1} + \omega_z\Delta t) + (1 - \alpha)\psi_{nb} \quad (21)$$

where the subscript k represents the current interaction, $k - 1$ the previous interaction. Values for α and, consequently, for $1 - \alpha$ are chosen according to the analyst's experience. In this work, it was used $\alpha = 0.95$, as found in most literature references. Then, the rotation matrix, Eq. 12, can be used again.

3.1.4 Kalman Filter

The Kalman filter can be used to estimate quantities using all readings of the sensor axis contributions within the IMU. All the distributions are considered Gaussians. In an integrated navigation system as an IMU, the first estimate is provided directly by the inertial navigation system, or system model, rate gyros in this work. The second estimate, the measurement or sensor model, is provided by the navigation aid, accelerometers for roll and pitch, and magnetometers for yaw angles. Romaniuk and Gosiewski (2014), Liu *et al.* (2014), Gui *et al.* (2015) used this approach in their works and have observed proper noise reduction on the orientation results.

The expressions for the Kalman filter are:

$$x_k = Fx_{k-1} + Bu_k + w_k \quad (22)$$

$$z_k = Hx_k + v_k \quad (23)$$

where w_k is a process noise and v_k is a measurement noise, u_k is the control input, given by the rate gyro signal, x_k is the system state matrix at time k :

$$x_k = \begin{bmatrix} \theta \\ b \end{bmatrix} \quad (24)$$

being θ the angle and b the rate gyro drift bias. The matrix F is called state transition matrix. For the IMU composed by three-axis rate gyros, accelerometers and magnetometers, F can be written as:

$$F = \begin{bmatrix} 1 & -\Delta t \\ 0 & 1 \end{bmatrix} \quad (25)$$

B is the control matrix,

$$B = \begin{bmatrix} \Delta t \\ 0 \end{bmatrix} \quad (26)$$

Also, z_k is the measurement output and H is the measurement matrix. As the measurement is from the accelerometers/magnetometers, H is defined as

$$H = [1 \ 0] \quad (27)$$

In the filter prediction step, the best prediction of the state at time t_{k+1} is given by:

$$x_{k+1/k} = F_k x_{k/k} + b\omega_{k+1} \quad (28)$$

The covariance matrix is predicted forward in time using the expression:

$$P_{k+1/k} = F_k P_{k/k} F_k^T + Q \quad (29)$$

$P_{k+1/k}$ denotes the expected value of the covariance matrix at time t_{k+1} predicted at time t_k . Q , the system noise matrix, is set up according to the expected level of noise on the inertial measurements of linear acceleration and angular rate.

In the measurement update step, the estimates of the errors in the inertial navigation system states are derived using:

$$x_{k+1/k+1} = K_{k+1} y_{k+1} \quad (30)$$

where,

$$y_{k+1} = z_{k+1} - Hx_{k+1/k} \quad (31)$$

and the covariance matrix is updated as

$$P_{k+1/k+1} = [I - K_{k+1} H_{k+1}] P_{k+1/k} \quad (32)$$

where the Kalman gain K is:

$$K_{k+1} = P_{k+1/k+1} H_{k+1}^T [H_{k+1} P_{k+1/k} H_{k+1}^T + R]^{-1} \quad (33)$$

where R is the measurement noise matrix.

4. RESULTS

The results from the signal processing will be presented, regarding the IMU orientation calculated through the rate gyros integration, quaternions, complementary filter, and Kalman filter. Once the orientation is known, the acceleration vector was transformed to the NED frame and also presented.

The purpose of this work is to evaluate only orientation, so simple rotation movements in the three directions (roll, pitch, and yaw) were made to present the method. It was conducted one movement in each axis, being first in the positive direction and then in the negative direction of rotation.

4.1 IMU Outputs

For accelerometers and rate gyros calibration, the offsets were calculated through the averages of the data obtained for the stationary sensor. These offset values were subtracted from the values read in the sensors.

For the magnetometer calibration, only the hard iron offset was correct, since a distortion has not been observed, that is, the result is a circle, not an ellipse. The values taken before and after the magnetometer calibration are presented in Figure 3. The magnetic field values after calibration are circle-shaped and zero-centered.

Applying the offset correction, related to the calibration, the raw values were divided by the sensitivity (gain), being 16384 for the accelerometer, which was also multiplied by 9.81 to obtain the results in m/s^2 ; 131 for rate gyro and; 1370 magnetometer. The results obtained are presented below, Figure 4, and the acquisition frequency is 250 Hz. It is evident the noisy signal and, to deal with this, the moving mean was applied to all data. The moving mean applied to the rate gyros signals is exposed in Figure 5. From these results, it is possible to calculate the IMU time orientation.

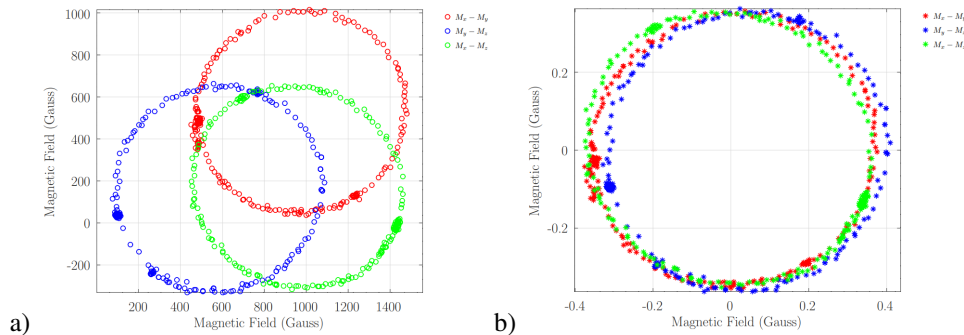


Figure 3. Magnetic field a) before and b) after hard iron compensation.

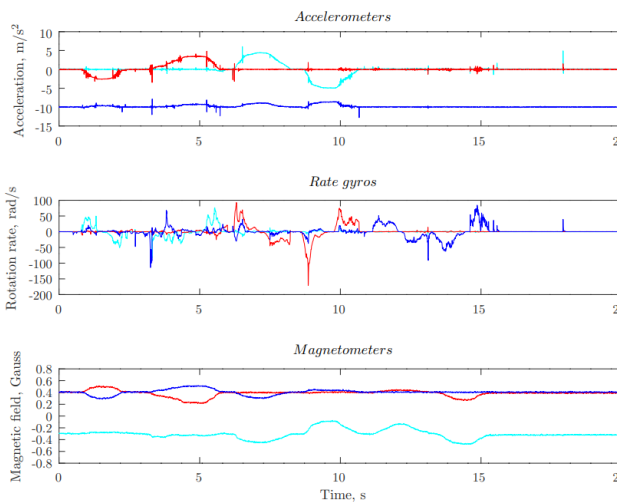


Figure 4. Time history of the IMU data (x axis in red, y axis in cyan and z axis in blue).

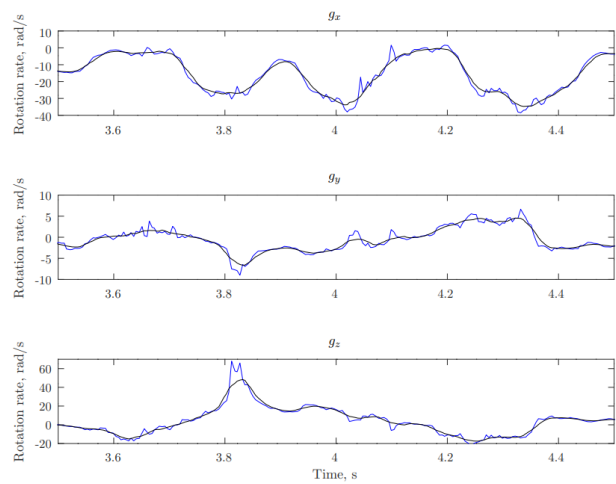


Figure 5. Rate gyros output without (blue line) and with moving mean filter (black line).

4.2 IMU Orientation

After treating the signal from high-frequency noises, the orientation was calculated, based on the equations presented in Sections 2 and 3. The magnetic declination considered is -0.34 rad in Joinville, Santa Catarina.

The Euler angles calculated using accelerometers, rate gyros, magnetometers, and the complementary filter are shown in Figure 6. It is possible to notice a noisy signal in the angles calculated with the accelerometers and magnetometers because these sensors are unstable to any kind of movement. Results from the rate gyros integration present a drift, due to dead reckoning, which is remarkable even in a few seconds of reading. Both noise and drift issues were solved when the complementary filter was applied.

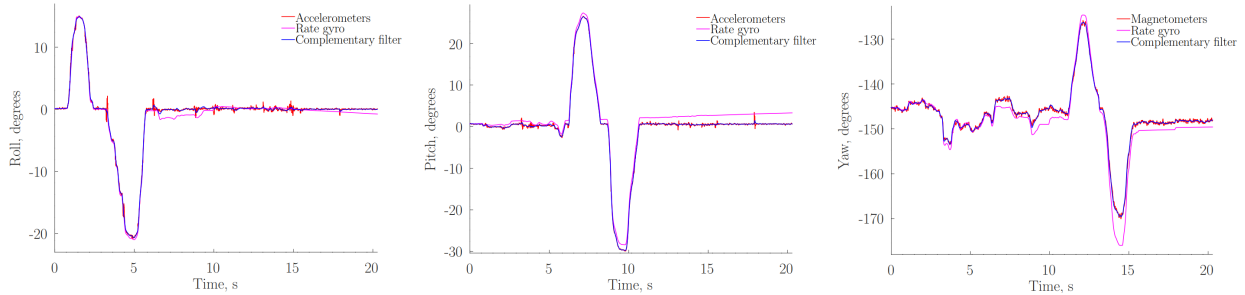


Figure 6. Time history for roll, pitch and yaw angles.

As an illustration, in Figure 7 may be seen the IMU (blue rectangle) orientated according to the reading at a specific time.

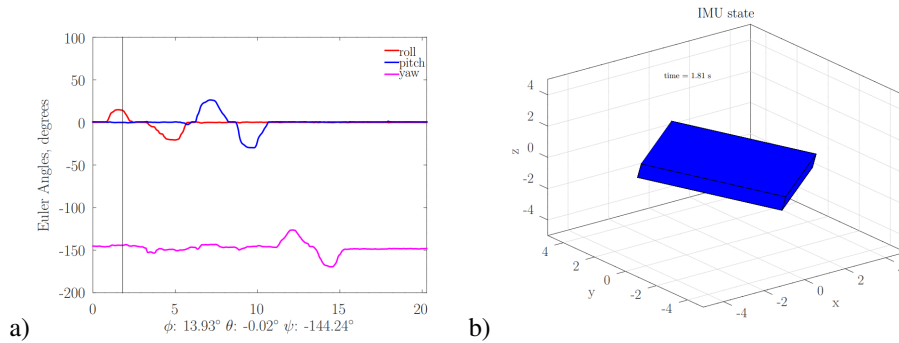


Figure 7. Illustration of the IMU orientation.

4.2.1 Comparison Between Methods

Complementary filter was calculated using a coefficient equal to 0.95 for rate gyros and 0.05 for accelerometers and magnetometers angles results. For the Kalman filter, measurement noise was considered equal to 0.03 (twice the accelerometer noise from datasheet) and a process noise of $0.001\Delta t$.

In Figure 8, roll, pitch, and yaw angles are presented, respectively, where the complementary filter, Kalman filter, and quaternions are compared. Although quaternions are a form of representation the rotation angles and not a filter, it ends up acting as one, creating a smoother transition between orientations. Then, as the quaternion, in this approach, uses only the rotation rate vectors, it is noticed the drift in the orientation angles.

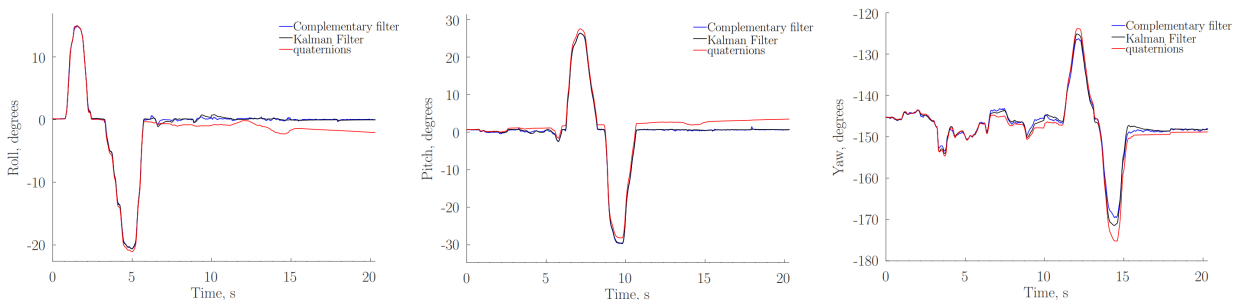


Figure 8. Time history for roll, pitch and yaw angles using sensor fusion and quaternions.

Results for complementary and Kalman filters are very similar, but differences can be seen when enlarging the graphic, see Figure 9. Then, the Kalman filter minimizes the sensors' noises even more than the complementary filter, which is positive especially when some control system is needed to correct the movement, for example. Quaternions are not noisy

but present the drift problem. A good procedure can be made using the Kalman filter for quaternion-based orientation approach, and that can be done in future works.

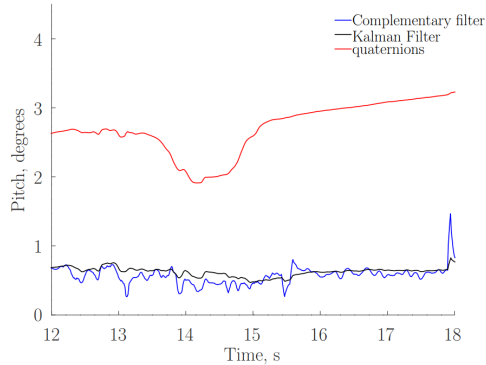


Figure 9. Zoom in on the pitch angle graphic.

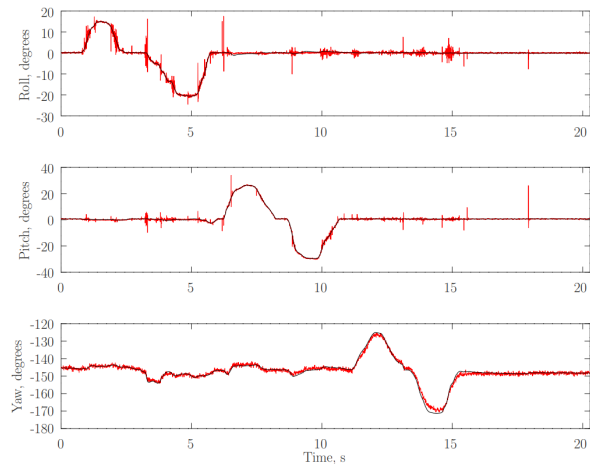


Figure 10. Comparison between sensors only (red line) and treated signal (black line).

The last comparison was done analyzing the orientation coming from the sensors only, accelerometers and magnetometers, without moving mean, against the orientation signal treated with moving mean and Kalman filter, Figure 10. The noise decrease is visible after signal treatment. Small deviations can generate big problems in signal expansions, as in successive multiplications and integration, leaving no doubt that a filtered signal will bring better results in future parameters coming from the orientations. After all, calculating orientations is only the first step in navigation instrumentation, but it is also an essential step.

4.3 Accelerations in NED frame

Having the orientations of the sensor defined, it is possible to transform any sensor signal to the Earth frame, also named NED (north, east, down). An important data is the acceleration, through which can be obtained the velocity and displacement data of the body. Accelerations transformation from sensor frame to NED frame, using the rotation matrix with Euler angles found with Kalman filter, are presented in Figure 11.

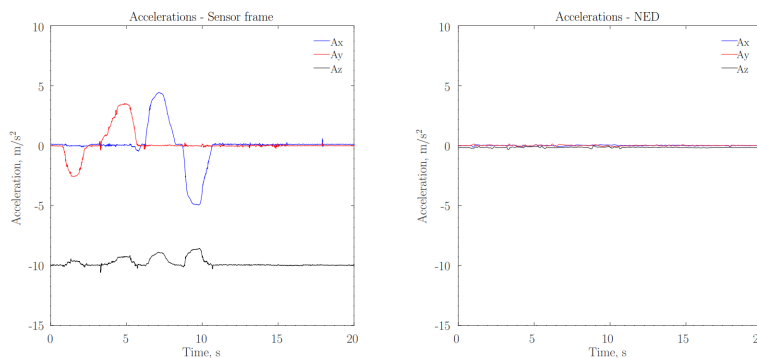


Figure 11. Acceleration signals in sensor and NED frames.

With this graphic can be noticed that the IMU is not moving relative to Earth, only rotating, and the NED accelerations are null. Also, noises are observed, and these can generate problems when the signals are integrated in time to obtain velocity and reintegrated to obtain the position, drift issues. Then, to have the position, the signal can be treated with a filter again but for that, it is necessary an external position measurement, which is not possible with only this IMU.

5. CONCLUSIONS

Signals coming from a low-cost IMU were read and treated in this work. Accelerometers and magnetometers signals are noisy, and rate gyros signals present drift. Combining the outputs of these sensors can lead to better results. Complementary and Kalman filters were applied to the Euler angles, in addition to values calculated directly by accelerometers, magnetometers, and rate gyros.

In the first approach, a complementary filter with accelerometers, magnetometers, and rate gyros present a very good result, minimizing the noise and drift problems. Quaternions are another approach to find orientation and, when using only rotation rates, the results are not noisy but present drift. For more accurate results, the Kalman filter can be applied. It requires exhausting work and a careful choice of parameters, but once tested and validated, it filters the signal even more clearly. All the methods used need the angles initialization to start the algorithm, and for that, calibrated accelerometers and magnetometers are essentials.

Kalman filter, with the parameters used, proved to be the best method to predict orientation reducing noise and drift. On the other hand, the complementary filter is much easier to implement and also present suitable results. The choice between each procedure will depend on the available time to perform the manipulations and tests.

For future works, integration in the acceleration vector can be made to find the position and see which method is the best for that, where a position sensor will be needed, possibly a GNSS. Also, a Kalman filter for quaternion-based orientation estimation can be applied to see the differences when the output is Euler angles and when it is quaternions. Tests using different IMUs can also be done, to compare commercial and low-cost IMU performances.

6. REFERENCES

- Barrera, F., Sampaio, R., Munoz, D. and Llanos, C.H., 2018. "A Study of Attitude and Heading Determination through an EKF-based Sensor Fusion for Inertial Measurement Units (IMUs)". doi:10.26678/abcm.cobem2017.cob17-1859.
- Driessen, S., Janssen, N., Wang, L., Palmer, J. and Nijmeijer, H., 2018. "Experimentally Validated Extended Kalman Filter for UAV State Estimation Using Low-Cost Sensors". *IFAC-PapersOnLine*, Vol. 51, No. 15, pp. 43–48. ISSN 2405-8963. 18th IFAC Symposium on System Identification SYSID 2018.
- Groves, P.D., 2015. "Principles of gnss, inertial, and multisensor integrated navigation systems, [book review]". *IEEE Aerospace and Electronic Systems Magazine*, Vol. 30, No. 2, pp. 26–27.
- Gui, P., Tang, L. and Mukhopadhyay, S., 2015. "Mems based imu for tilting measurement: Comparison of complementary and kalman filter based data fusion". In *2015 IEEE 10th conference on Industrial Electronics and Applications (ICIEA)*. IEEE, pp. 2004–2009.
- Lavieri, R.S., 2011. "Inertial navigation methods applied to underwater launches." *Master Dissertation*.
- Liu, Y., Guo, S., Shi, L., Xing, H., Hou, X., Liu, H., Hu, Y., Xia, D. and Li, Z., 2019. "Multi-Sensor Fusion Based Localization System for an Amphibious Spherical Robot". *Proceedings of 2019 IEEE International Conference on Mechatronics and Automation, ICMA 2019*, pp. 2523–2528. doi:10.1109/ICMA.2019.8816345.
- Liu, Y., Noguchi, N. and Ishii, K., 2014. "Development of a low-cost imu by using sensor fusion for attitude angle estimation". *IFAC Proceedings Volumes*, Vol. 47, No. 3, pp. 4435–4440.
- Morooka, C.K. and Tsukada, R.I., 2013. "Experiments with a steel catenary riser model in a towing tank". *Applied Ocean Research*, Vol. 43, pp. 244–255.
- Mukundan, H., Hover, F. and Triantafyllou, M., 2010. "A systematic approach to riser VIV response reconstruction". *Journal of fluids and structures*, Vol. 26, No. 5, pp. 722–746.
- Pesce, C. and Martins, C., 2005. "Numerical computation of riser dynamics". *Numerical Models in Fluid-Structure Interaction*, pp. 253–309. doi:10.2495/978-1-85312-837-0/07.
- Ramos, R. and Pesce, C.P., 2004. "A consistent analytical model to predict the structural behavior of flexible risers subjected to combined loads". *Journal of Offshore Mechanics and Arctic Engineering*, Vol. 126, No. 2, pp. 141–146. ISSN 08927219. doi:10.1115/1.1710869.
- Romaniuk, S. and Gosiewski, Z., 2014. "Kalman filter realization for orientation and position estimation on dedicated processor". *acta mechanica et automatica*, Vol. 8, No. 2, pp. 88–94.
- Vissière, D., Martin, A. and Petit, N., 2007. "Using distributed magnetometers to increase IMU-based velocity estimation into perturbed area". In *2007 46th IEEE Conference on Decision and Control*. IEEE, pp. 4924–4931.

7. RESPONSIBILITY NOTICE

The authors are solely responsible for the printed material included in this paper.